Electronic Supplementary Material (ESI) for Dalton Transactions.
This journal is © The Royal Society of Chemistry 2023

Supporting Information

Structure and magnetic properties of an amine-templated one-dimensional cobalt-fluoro-sulfate containing Co_4F_4 Cubane & hydrogen evolution reaction (HER) performance of its derived carbon-wrapped $CoSe_2$ nanorods

Malaya K. Sahoo[ab], J. N. Behera[ab]*

[a] School of Chemical Science, National Institute of Science Education and Research (NISER) an OCC of Homi Bhabha National Institute (HBNI), Khurda, 752050, Odisha, India.

[b] Centre for Interdisciplinary Sciences (CIS), NISER, Khurda, 752050, Odisha, India.

E-mail: jnbehera@niser.ac.in

Electrochemical Calculations:

All electrochemical data are collected taking Ag/AgCl reference electrode and later converted to a reversible hydrogen electrode (RHE) scale by the following equation for comparative analysis and presentation.

$$E_{RHE} = E^{\circ}_{Ag/AgCl} + 0.059 \times pH + E_{Ag/AgCl}$$

Again, the intrinsic activity of the catalysts is compared by compensating the ohmic drop (iR) that suppresses the real activity of the catalyst due to the unavoidable series resistance of the solution and electrical contact using the following equation.[1]

$$E_{iR} = E - iR$$

Specific activity: The specific activity is the activity per unit electrochemically accessible surface area of the catalyst. It is the plot of the current density vs working electrode potential in the RHE scale. Here the current density is obtained by normalizing the experimental LSV current to the electrochemically accessible surface.

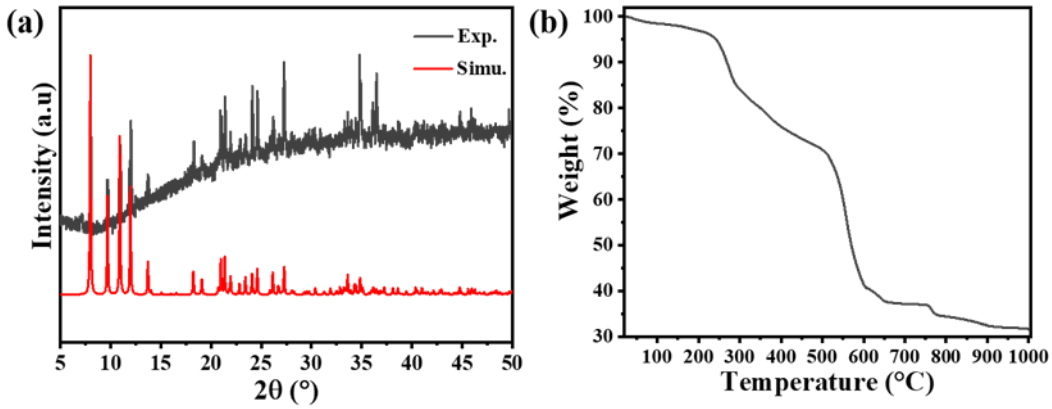

Figure S1. (a) Simulated and experimental powder pattern and (b) TGA spectrum of the Cubane chain.

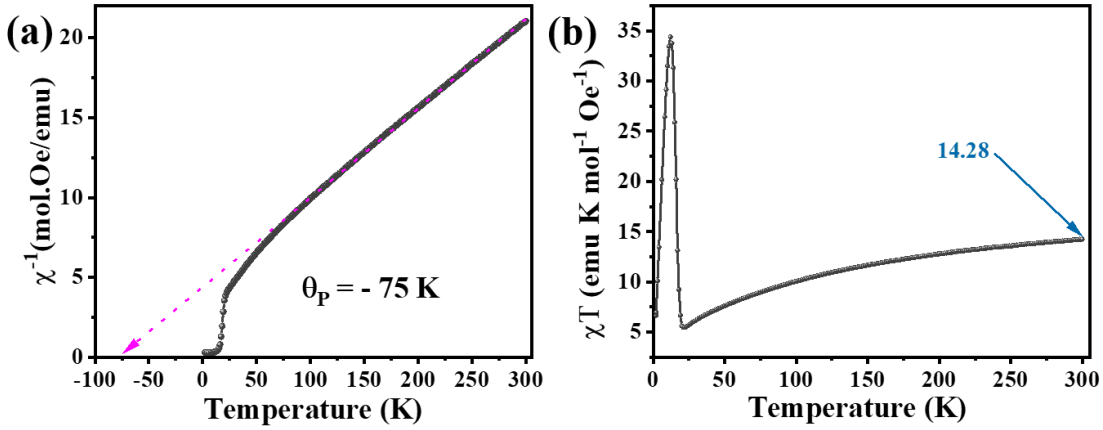

Figure S2. (a) Curie-Weiss fitting of the reciprocal susceptibility, (b) variation of observed magnetic moment with temperature for the Cubane chain.

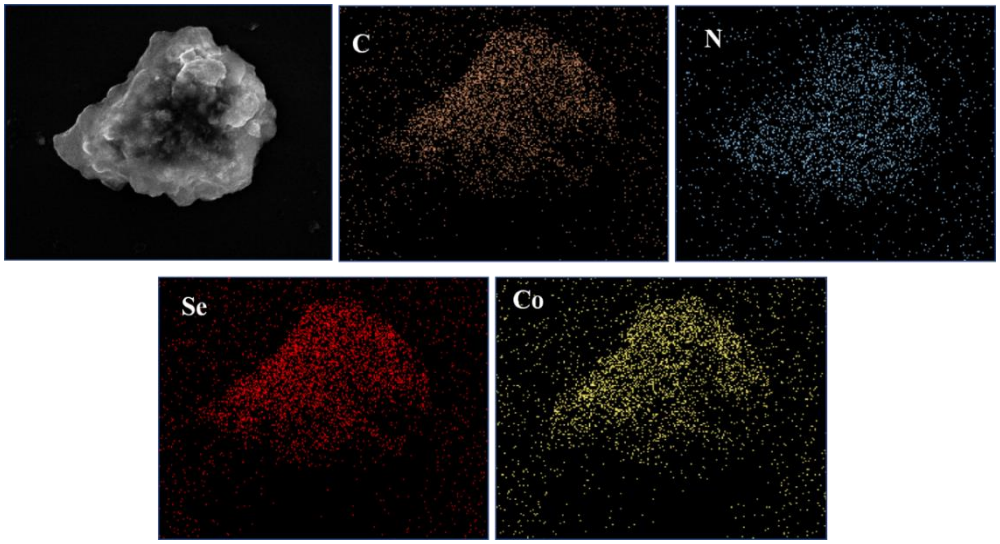

Figure S3. EDAX elemental mapping of $CoSe_2$@ST shows the uniform distribution of Co, Se, and the rich nitrogen and carbonaceous matrix.

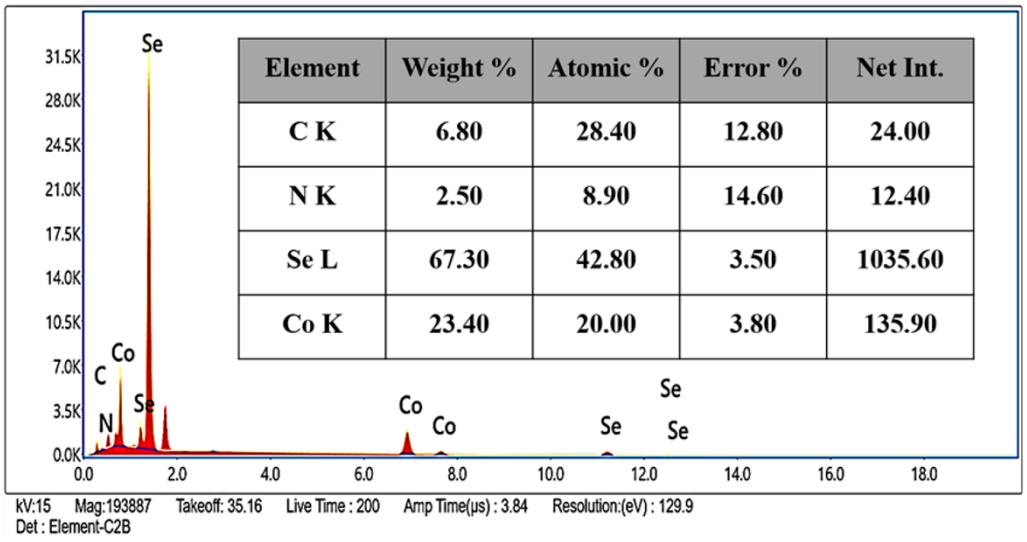

Element	Weight %	Atomic %	Error %	Net Int.
C K	6.80	28.40	12.80	24.00
N K	2.50	8.90	14.60	12.40
Se L	67.30	42.80	3.50	1035.60
Co K	23.40	20.00	3.80	135.90

Figure S4. EDS spectrum and elemental table with the elemental percentage in $CoSe_2$@ST.

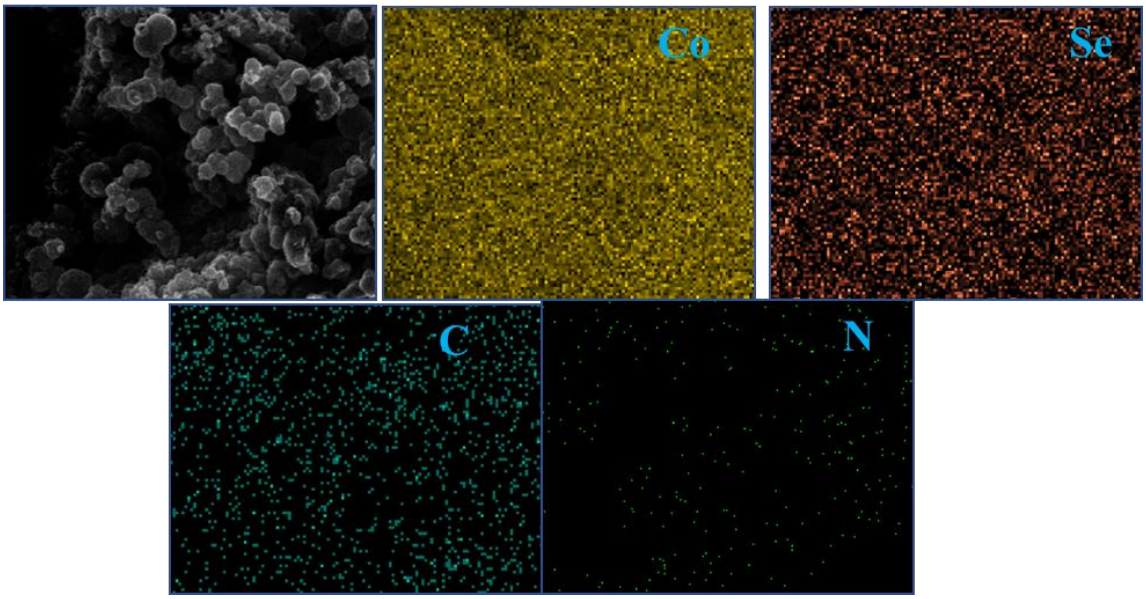

Figure S5. EDAX elemental mapping of $CoSe_2$@HT shows the uniform distribution of Co, Se, and the presence of a very minute quantity of nitrogen and carbon.

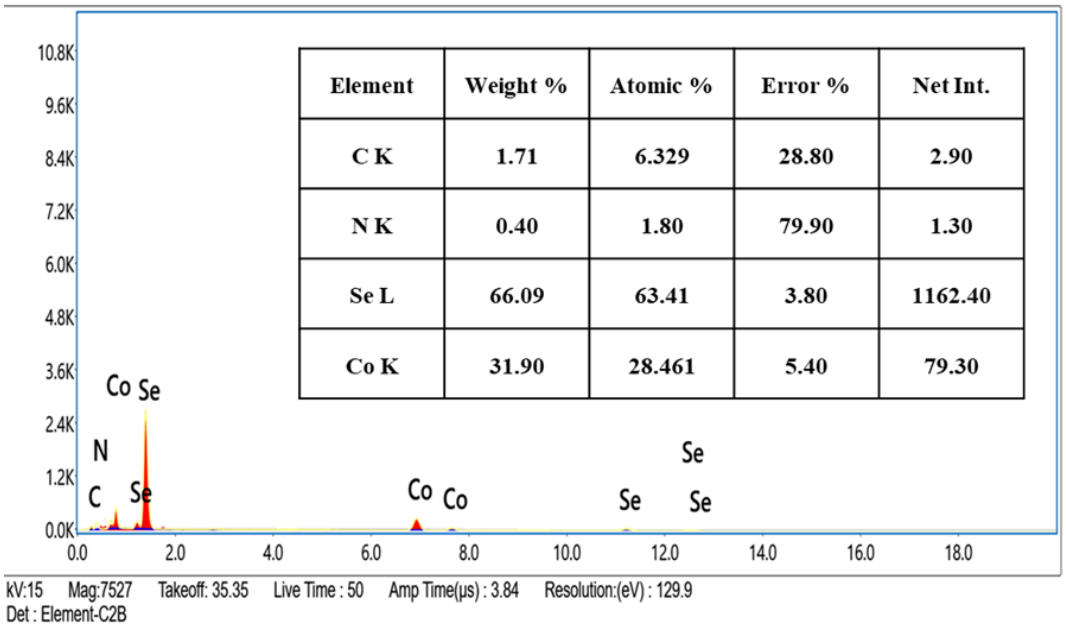

Element	Weight %	Atomic %	Error %	Net Int.
C K	1.71	6.329	28.80	2.90
N K	0.40	1.80	79.90	1.30
Se L	66.09	63.41	3.80	1162.40
Co K	31.90	28.461	5.40	79.30

Figure S6. EDS spectrum and elemental table with the elemental percentage in $CoSe_2$@HT.

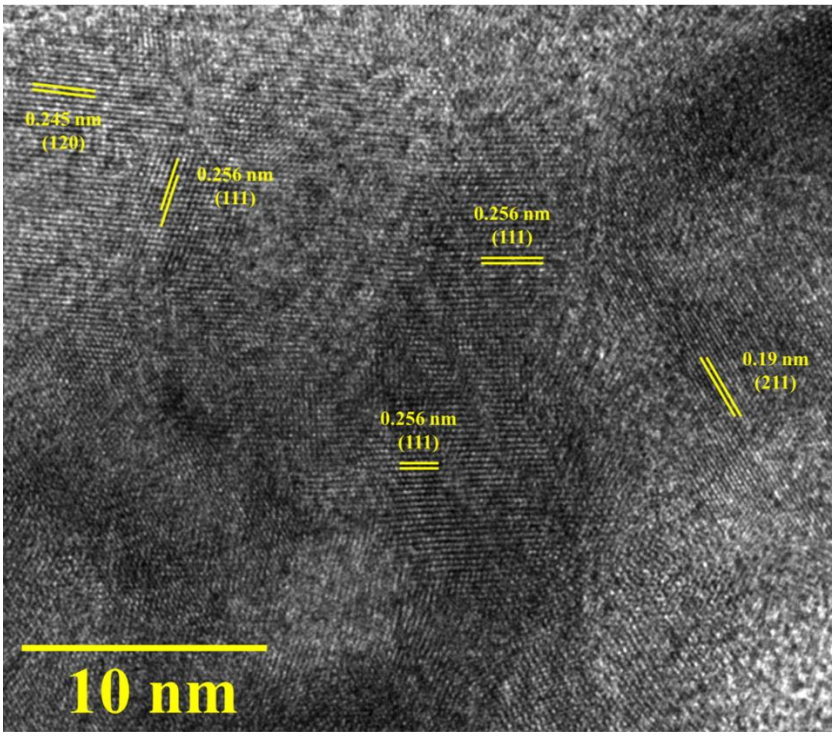

Figure S7. HR-TEM showing the lattice fringes of $CoSe_2$ in $CoSe_2$@ST.

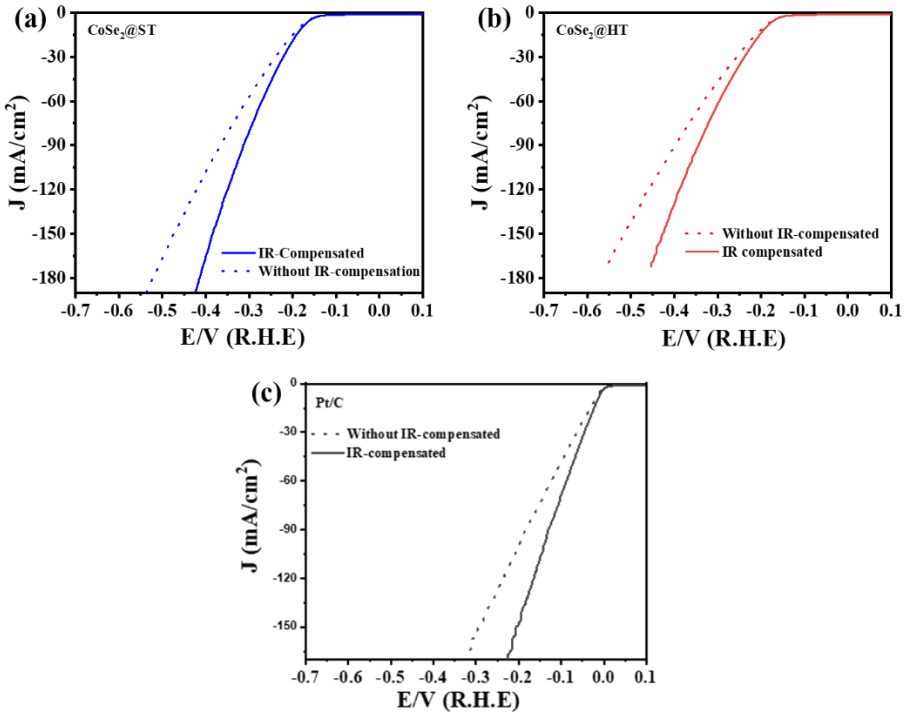

Figure S8. Ohmic drop (iR) uncompensated LSVs of all the catalysts.

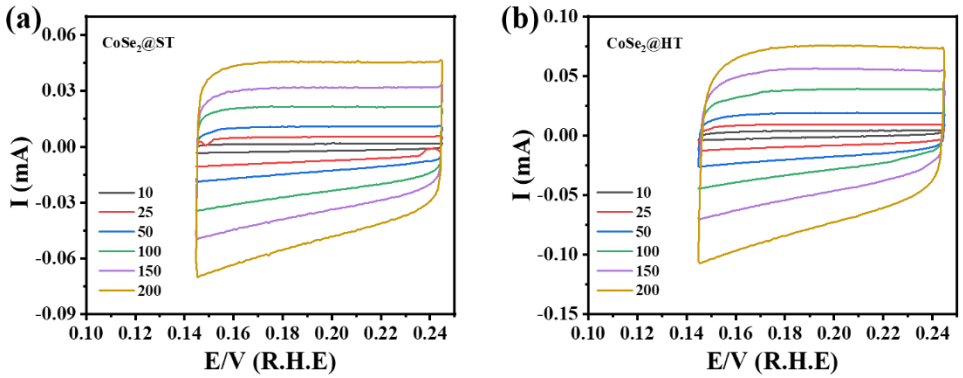

Figure S9. Cyclic voltammograms at different scan rates in the EDLC region.

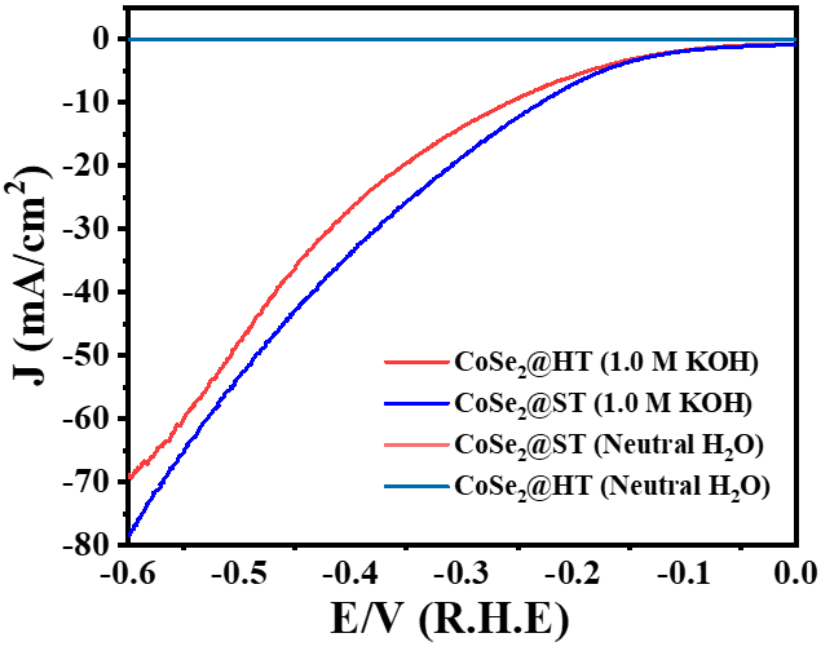

Figure S10. Linear-sweep voltammograms of the catalysts in 1.0 M KOH and neutral water.

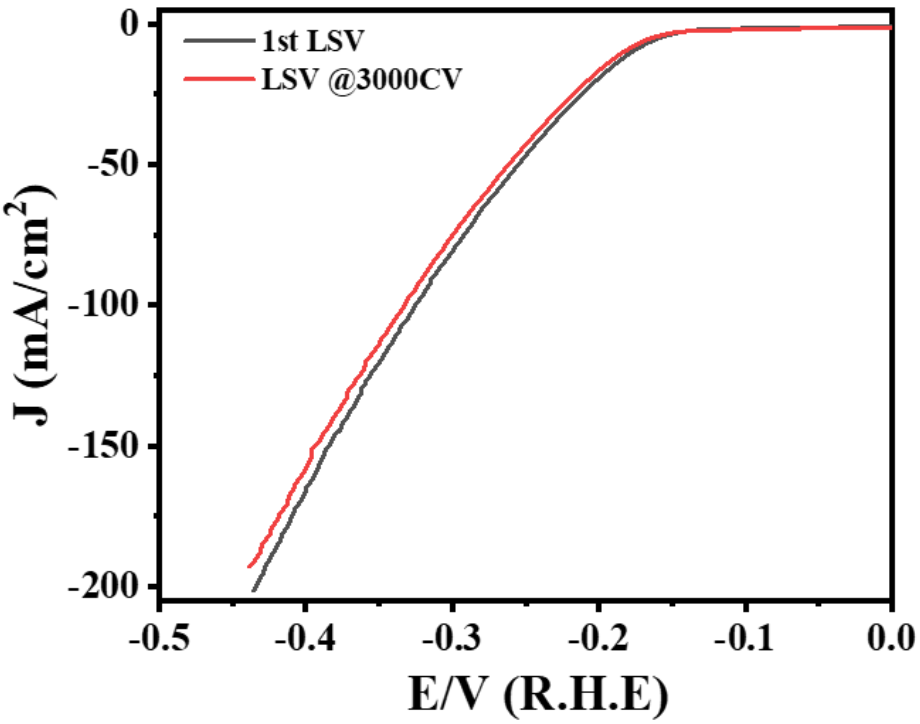

Figure S11. Linear-sweep voltammograms of the CoSe2@ST before and after 3000 continuous CV cycles.

Table S1. Selected bond lengths for the 1D Cubane chain.

Atom	Atom	Length/Å	Atom	Atom	Length/Å
Co2	F2	2.092(7)	Co1	O1	2.039(10)
Co2	F2^1	2.105(8)	Co1	N1	2.042(11)
Co2	F1	2.097(8)	F2	Co2^1	2.105(8)
Co2	O5	2.096(9)	F1	Co1^1	2.077(9)
Co2	O2	2.078(10)	Co1	F1^1	2.077(9)
Co2	N3	2.045(11)	Co1	O6	2.079(9)
Co1	F2	2.117(8)	Co1	O1	2.039(10)
Co1	F1	2.113(8)	Co1	N1	2.042(11)

Table S2. The selected bond angle of the 1D Cubane chain.

Atom	Atom	Atom	Angle/˚		Atom	Atom	Atom	Angle/˚
F2	Co2	$F2^1$	81.8(3)		N3	Co2	O2	95.4(4)
F2	Co2	F1	82.3(3)		$F1^1$	Co1	F2	77.3(3)
F2	Co2	O5	87.9(3)		F1	Co1	F2	81.3(3)
F1	Co2	$F2^1$	77.1(3)		$F1^1$	Co1	F1	80.7(4)
O5	Co2	$F2^1$	88.4(3)		$F1^1$	Co1	O6	86.8(4)
O5	Co2	F1	163.5(3)		O6	Co1	F2	163.0(3)
O2	Co2	F2	86.3(4)		O6	Co1	F1	90.4(4)
O2	Co2	$F2^1$	164.3(3)		O1	Co1	F2	93.5(4)
O2	Co2	F1	91.3(4)		Co2	F2	$Co2^1$	97.1(3)
O2	Co2	O5	101.3(4)		$Co2^1$	F2	Co1	101.9(3)
N3	Co2	$F2^1$	96.8(4)		Co2	F2	Co1	96.7(3)
N3	Co2	F2	178.0(4)		Co2	F1	Co1	96.6(3)
N3	Co2	F1	98.7(4)		$Co1^1$	F1	Co2	103.5(4)
N3	Co2	O5	90.8(4)		$Co1^1$	F1	Co1	97.9(4)
O1	Co1	$F1^1$	163.6(4)		N1	Co1	F2	96.2(4)
O1	Co1	F1	84.6(4)		N1	Co1	$F1^1$	98.8(4)
O1	Co1	O6	100.4(5)		N1	Co1	F1	177.5(5)
O1	Co1	N1	95.6(5)		N1	Co1	O6	92.0(5)

Table S3 Electrochemical HER activity comparison with previous reports.

SL No.	Catalyst	Overpotential @10 mA/cm^2	Tafel Slope	Reference
1	$CoSe_2$|CoP/CFP	140	42	[2]
	$CoSe_2$/CFP	219	44	
2	$CoSe_2$-CNT	174	37.8	[3]
3	$Mn_{0.05}Co_{0.95}Se_2$	174	36	[4]
	$CoSe_2$ Nanosheet	250	52	
4	$CoSe_2$@NC	184	58.4	[5]
5	MOF-$CoSe_2$	150@onset	42	[6]
		330@80		
6	$CoSe_2$	272	55	[7]
7	Ru-CoSe-NC	152	37	[8]
	CoSe-NC	228	46	
8	$CoSe_2$@N/C-CNT	185	98	[9]
9	p-$CoSe_2$@HC	171.7	45.7	[10]

10	$CoSe_2$	137	42.1	[11]
11	$MoSe_2/CoSe_2$ hybrid	129	38.2	[12]
12	o-$CoSe_2$	300		[13]
13	$Ni_{0.33}Co_{0.67}Se_2$	65	35	[14]
14	o-$CoSe_2$-NC	147	39.8	[15]
15	Cobalt selenide films	135	62	[16]
16	meso-CoSSe-12h	110	52	[17]
17	$CoSe_2$/C	253	46	[18]
18	MOF-D $CoSe_2$	195	43	[19]
19	$CoSe_2$@HT	189	57	**Present Work**
20	$CoSe_2$@ST	177	48	

References

(1) Anantharaj, S.; Noda, S. IR Drop Correction in Potentiostatic Electrocatalysis: Everything One Needs to Know! *J. Mater. Chem. A* **2022**, 9348–9354. https://doi.org/10.1039/D2TA01393B.

(2) Bose, R.; Kim, T.-H.; Koh, B.; Jung, C.-Y.; Yi, S. C. Influence of Phosphidation on CoSe2 Catalyst for Hydrogen Evolution Reaction. *ChemistrySelect* **2017**, *2* (33), 10661–10667. https://doi.org/https://doi.org/10.1002/slct.201702172.

(3) Kim, J. K.; Park, G. D.; Kim, J. H.; Park, S.-K.; Kang, Y. C. Rational Design and Synthesis of Extremely Efficient Macroporous CoSe2–CNT Composite Microspheres for Hydrogen Evolution Reaction. *Small* **2017**, *13* (27), 1700068. https://doi.org/https://doi.org/10.1002/smll.201700068.

(4) Liu, Y.; Hua, X.; Xiao, C.; Zhou, T.; Huang, P.; Guo, Z.; Pan, B.; Xie, Y. Heterogeneous Spin States in Ultrathin Nanosheets Induce Subtle Lattice Distortion To Trigger Efficient Hydrogen Evolution. *J. Am. Chem. Soc.* **2016**, *138* (15), 5087–5092. https://doi.org/10.1021/jacs.6b00858.

(5) Do, H. H.; Le, Q. Van; Cho, J. H.; Ahn, S. H.; Kim, S. Y. Comparative Study on Hydrogen Evolution Reaction of Various Cobalt-Selenide-Based Electrocatalysts. *Int. J. Energy Res.* **2023**, *2023*, 6016603. https://doi.org/10.1155/2023/6016603.

(6) Lin, J.; He, J.; Qi, F.; Zheng, B.; Wang, X.; Yu, B.; Zhou, K.; Zhang, W.; Li, Y.; Chen, Y. In-Situ Selenization of Co-Based Metal-Organic Frameworks as a Highly Efficient Electrocatalyst for Hydrogen Evolution Reaction. *Electrochim. Acta* **2017**, *247*, 258–264. https://doi.org/https://doi.org/10.1016/j.electacta.2017.06.179.

(7) McCarthy, C. L.; Downes, C. A.; Schueller, E. C.; Abuyen, K.; Brutchey, R. L. Method for the Solution Deposition of Phase-Pure CoSe2 as an Efficient Hydrogen Evolution Reaction Electrocatalyst. *ACS Energy Lett.* **2016**, *1* (3), 607–611. https://doi.org/10.1021/acsenergylett.6b00246.

(8) Wang, M.; Dang, Z.; Prato, M.; Petralanda, U.; Infante, I.; Shinde, D. V; De Trizio, L.; Manna, L. Ruthenium-Decorated Cobalt Selenide Nanocrystals for Hydrogen Evolution. *ACS Appl. Nano Mater.* **2019**, *2* (9), 5695–5703. https://doi.org/10.1021/acsanm.9b01205.

(9) Ding, H.; Xu, G.; Zhang, L.; Wei, B.; Hei, J.; Chen, L. A Highly Effective Bifunctional Catalyst of Cobalt Selenide Nanoparticles Embedded Nitrogen-Doped Bamboo-like Carbon Nanotubes toward Hydrogen and Oxygen Evolution Reactions Based on Metal-Organic Framework. *J. Colloid Interface Sci.* **2020**, *566*, 296–303. https://doi.org/https://doi.org/10.1016/j.jcis.2020.01.096.

(10) Yang, S. H.; Park, G. D.; Kim, J. K.; Kang, Y. C. New Strategy to Synthesize Optimal Cobalt Diselenide@hollow Mesoporous Carbon Nanospheres for Highly Efficient Hydrogen Evolution Reaction. *Chem. Eng. J.* **2021**, *424*, 130341. https://doi.org/https://doi.org/10.1016/j.cej.2021.130341.

(11) Kong, D.; Wang, H.; Lu, Z.; Cui, Y. CoSe2 Nanoparticles Grown on Carbon Fiber Paper: An Efficient and Stable Electrocatalyst for Hydrogen Evolution Reaction. *J. Am. Chem. Soc.* **2014**, *136* (13), 4897–4900. https://doi.org/10.1021/ja501497n.

(12) Wang, Y.; Jian, C.; He, X.; Liu, W. Self-Supported Molybdenum Selenide Nanosheets Grown on Urchin-like Cobalt Selenide Nanowires Array for Efficient Hydrogen Evolution. *Int. J. Hydrogen Energy* **2020**, *45* (24), 13282–13289. https://doi.org/https://doi.org/10.1016/j.ijhydene.2020.03.017.

(13) Zhou, Z.; Yang, Y.; Hu, L.; Zhou, G.; Xia, Y.; Hu, Q.; Yin, W.; Zhu, X.; Yi, J.; Wang, X. Phase Control of Cobalt Selenide: Unraveling the Relationship Between Phase Property and Hydrogen Evolution Catalysis. *Adv. Mater. Interfaces* **2022**, *9* (29), 2201473. https://doi.org/https://doi.org/10.1002/admi.202201473.

(14) Xia, C.; Liang, H.; Zhu, J.; Schwingenschlögl, U.; Alshareef, H. N. Active Edge Sites Engineering in Nickel Cobalt Selenide Solid Solutions for Highly Efficient Hydrogen

Evolution. *Adv. Energy Mater.* **2017**, *7* (9), 1602089. https://doi.org/https://doi.org/10.1002/aenm.201602089.

(15) Sun, J.; Li, J.; Li, Z.; Hu, X.; Bai, H.; Meng, X. Phase Transition in Cobalt Selenide with a Greatly Improved Electrocatalytic Activity in Hydrogen Evolution Reactions. *ACS Sustain. Chem. Eng.* **2022**, *10* (12), 4022–4030. https://doi.org/10.1021/acssuschemeng.2c00449.

(16) Carim, A. I.; Saadi, F. H.; Soriaga, M. P.; Lewis, N. S. Electrocatalysis of the Hydrogen-Evolution Reaction by Electrodeposited Amorphous Cobalt Selenide Films. *J. Mater. Chem. A* **2014**, *2* (34), 13835–13839. https://doi.org/10.1039/C4TA02611J.

(17) Dutta, B.; Wu, Y.; Chen, J.; Wang, J.; He, J.; Sharafeldin, M.; Kerns, P.; Jin, L.; Dongare, A. M.; Rusling, J.; Suib, S. L. Partial Surface Selenization of Cobalt Sulfide Microspheres for Enhancing the Hydrogen Evolution Reaction. *ACS Catal.* **2019**, *9* (1), 456–465. https://doi.org/10.1021/acscatal.8b02904.

(18) Tripathy, R. K.; Samantara, A. K.; Mane, P.; Chakraborty, B.; Behera, J. N. Cobalt Metal Organic Framework (Co-MOF) Derived CoSe2/C Hybrid Nanostructures for the Electrochemical Hydrogen Evolution Reaction Supported by DFT Studies. *New J. Chem.* **2022**, *46* (6), 2730–2738. https://doi.org/10.1039/D1NJ05528C.

(19) Sahu, N.; Das, J. K.; Behera, J. N. Metal–Organic Framework (MOF) Derived Flower-Shaped CoSe2 Nanoplates as a Superior Bifunctional Electrocatalyst for Both Oxygen and Hydrogen Evolution Reactions. *Sustain. Energy Fuels* **2021**, *5* (19), 4992–5000. https://doi.org/10.1039/D1SE01112J.